Energy Reports 8 (2022) 2351–2362

Contents lists available at ScienceDirect

Energy Reports

journal homepage: www.elsevier.com/locate/egyr

Research paper

Energy, economic and environmental analysis of a BOG re-liquefaction process for an LNG carrier

Chulmin Hwang [a], Sungkyun Oh [b], Donghoi Kim [c], Truls Gundersen [d], Youngsub Lim [a,e,*]

[a] Department of Naval Architecture and Ocean Engineering, Seoul National University, 1 Gwanak-ro, Gwanak-gu, Seoul, 08826, Republic of Korea
[b] Department of Mechanical and Aerospace Engineering, Seoul National University, 1 Gwanak-ro, Gwanak-gu, Seoul, 08826, Republic of Korea
[c] SINTEF Energy Research, Sem Sælands vei 11, NO-7465, Trondheim, Norway
[d] Department of Energy and Process Engineering, Norwegian University of Science and Technology (NTNU), Kolbjørn Hejes Vei 1B, NO-7491, Trondheim, Norway
[e] Research Institute of Marine Systems Engineering, Seoul National University, 1 Gwanak-ro, Gwanak-gu, Seoul, 08826, Republic of Korea

ARTICLE INFO

Article history:
Received 26 October 2021
Received in revised form 19 December 2021
Accepted 13 January 2022
Available online xxxx

Keywords:
LNG carrier
Boil-off gas
Re-liquefaction
Optimization

ABSTRACT

Due to tighter environmental regulations, newly built liquefied natural gas (LNG) carriers are equipped with a re-liquefaction system to minimize combustion of surplus boil-off-gas (BOG). Thus, this paper comparatively analyzes the re-liquefaction system for a low-pressure gas injection engine according to the refrigerant (no external refrigerant or single mixed refrigerant) with three key performance indicators: energy, economic, and environmental aspects. For an energy efficiency analysis, we proposed several process alternatives and optimized them to minimize the specific power consumption required to liquefy BOG. In economic analysis, minimizing total annualized cost is the objective. For an environmental analysis, CO_2 emissions at each optimal point is calculated and comparatively analyzed. The results show that the process without external refrigerant has 10% better performance in terms of economy, while the single mixed refrigerant process is suitable in terms of energy efficiency (6%) and environmental (15%) impact.

1. Introduction

For the past decades, the continuously growing demand for liquefied natural gas (LNG) have stimulated the active development and operation of LNG carriers. In terms of their scale in 2019, the top three international LNG importers are Japan (76.9 Mt), China (61.7 Mt), and South Korea (40.1 Mt), which account for 50.3% of the total worldwide trade (354.7 Mt) (IGU, 2020). Due to most of the major consumers' geographical characteristics, LNG shipping is a crucial technology that still requires improvement to allow the possibly largest amount of LNG transport in a single voyage. For example, the thin flexible membrane tanker structure has been developed and optimized for the LNG storage tank to replace the spherical tanker array structure (Moss design), to offer a nearly 10% enhanced shipping capability (Man Diesel & Turbo, 2013).

Recently, due to the economic and environmental issues of boil-off gas (BOG) from LNG cargo, BOG re-liquefaction process systems have become an effective solution for LNG carriers (George et al., 2020; Romero Gómez et al., 2015). The challenging issue for LNG shipping is to maintain the LNG cargo in liquid phase by keeping the storage tank at a desired cryogenic temperature (< −160 °C) during the voyage. Although the LNG cargo tanks are well insulated, the partial evaporation of LNG in the storage tank is inevitable due to heat transfer from the ambient, causing the generation of BOG. BOG in the storage tank has to be properly monitored and removed from the tank to avoid internal tank pressure build up that can cause structural problems (e.g., explosions, fracture). Conventionally, excess BOG is merely burnt in a gas combustion unit (GCU), which results in cargo loss and also generation of large amounts of carbon dioxide (CO_2) and combustion pollutants. After the 74th international maritime organization (IMO) marine environment protection committee (MEPC 74) (Council of the European Union, 2019), the energy efficiency design index (EEDI) is strengthened to phase 3, in which CO_2 emissions should be reduced by 30% in 2022, and (provisionally) 70% reduction in 2050 for LNG carriers. As a result, reducing CO_2 emissions is one of the major issues while the design and operation of LNG carriers being conditioned by the stricter environmental regulations. One of the methods for complying with the intense regulation is re-liquefying BOG. With a re-liquefaction system being capable of recovering the excessive BOG, the re-liquefied BOG can be re-routed to be charged into the storage tank. This possesses the critical benefit of reducing CO_2 emissions and cargo loss.

* Correspondence to: Gwanak-ro, Gwanak-gu, Seoul, 08826, Republic of Korea.
E-mail address: s98thesb@snu.ac.kr (Y. Lim).

https://doi.org/10.1016/j.egyr.2022.01.098

Nomenclature

Roman letters

A	capacity of unit [-]
$ATCI$	annual total capital investment [$/yr]
$ATOC$	annual total operating cost [$/yr]
C	annual cost [$/yr]
E	energy value of burnt BOG [kJ/d]
F	factor [-]
i	interest rate [%]
K	coefficient [-]
LHV	lower heating value [kJ/kg]
$\dot{m}$	mass flow rate [kg/h]
N	number of cycles [cycle/yr]
n	service life of LNG carrier [yr]
P	power [kWh]
SPC	specific power consumption [kWh/kg LNG]
T	temperature [°C]
TAC	total annualized cost [$/yr]
TCI	total capital investment [$]
Y	product gas compositions [-]

Greek letters

ΔP	pressure drop [bar]
ΔT_{min}	minimum approach temperature [°C]

Abbreviations

BOG	boil-off gas
CAPEX	capital expenditure
CHE	cryogenic heat exchanger
DFDE	dual-fuel diesel electric
EEDI	energy efficiency design index
FGSS	fuel gas supply system
GCU	gas combustion unit
HP	high-pressure
IMO	international maritime organization
LNG	liquefied natural gas
LP	low-pressure
MEPC	marine environment protection committee
MMBTU	metric million british thermal unit
MR	mixed refrigerant
NER	no external refrigerant
PSO	particle swarm optimization
SFOC	specific fuel oil consumption
SMR	single mixed refrigerants

Subscripts

AUX	auxiliary engine
BM	bare module costs
BOG loss	boil-off-gas burnt in GCU
CO_2	carbon dioxide
comp	compressor
CTO	correlation from capital cost to operating cost
cw	cooling water
cycle	voyage cycle
Ext	extra expenses
GAS	vent gas
j	process unit
P	purchased cost
power consumption	total power consumption
PROP	propulsion engine
re-liquefied LNG	re-liquefied LNG through process

There have been numerous works attempting to integrate onboard re-liquefaction processes in conjunction with the gas injection engines. Recently, the newly-developed gas-injection engines have increasingly replaced the conventional engines due to their high efficiency (∼50% (Tu Huan et al., 2019)), geometric redundancy, and clean emission characteristics when combining with the BOG re-liquefaction system (Man Diesel & Turbo, 2013; Fernández et al., 2017). The LNG propulsion system can be classified into electrically driven (e.g., dual-fuel diesel electric (DFDE)) and mechanically driven (e.g., diesel, dual-fuel) types (Fernández et al., 2017). However, the electrically driven propulsion system is not favorable to be integrated with a re-liquefaction facility due to the high investment cost. In general, BOG re-liquefaction is subject to substantial economic burden, and thus, the high-investment cost for the DFDE makes it a less attractive option. Instead, the mechanically driven propulsion system with a re-liquefaction process is a common combination for LNG carriers, taking less space and the capital expenditure (CAPEX) compared to the DFDE based option. Conventionally, the two-stroke diesel engine with a re-liquefaction process is chosen for the main propulsion system (Fernández et al., 2017). MAN B&W (Man Diesel & Turbo, 2012) has developed the two-stroke gas engine supplied with pressurized BOG at nearly 300 bar with a re-liquefaction system. By directly-injecting natural gas at a high pressure, the engine outperforms on pollutant emissions while it benefits from the high thermal efficiency in comparison to the two-stroke diesel counterpart. Methods for delivering high-pressure fuel streams have also been applied including the multi-stage gas compressors (Burckhardt Compression AG, 2016). The high fuel boosting pressure allows for an integrated BOG refrigeration design as a widely adopted choice for re-liquefaction processes (Tan et al., 2016). The efficiency of re-liquefaction in conjunction with high-pressure (HP) systems has been investigated by Romero Gómez et al. (2015), who performed a detailed exergy and energy analyses. Tan et al. (2018) proposed a novel cycle design for efficiency enhancement in high-pressure systems. The energy-efficient compact re-liquefaction system design for high-pressure gas fueled ships has been carried out by Kwak et al. (2018). Moreover, our recent studies (Kim et al., 2019; Hwang and Lim, 2018) presented economic optimization of the re-liquefaction process installation in HP-based LNG carriers.

Currently, the low-pressure (LP) gas injection engine is becoming another option for the propulsion system due to its clean combustion technology, reliable design, and lower installation and operating cost. For example, Tu Huan et al. (2019) showed that the nitrogen oxide (NO_x) level in LP exhaust without post-treatment drops by 25% compared to the HP reference case, and CAPEX associated with the fuel gas supply system is significantly lower (60%–70%) in the LP system compared with the HP system. However, integrated analysis and optimization studies of the propulsion system and the re-liquefaction facilities are sparsely available. George et al. (2020) defined the concept of re-liquefaction efficiency and presented an efficiency-based assessment for various vessel speeds. Choi (2018) performed a

detailed exergy analysis in a full/partial re-liquefaction process based on a low-pressure facility (16 bar) for efficiency improvement. These studies did not clearly show the three key points required for a BOG re-liquefaction process. First, some research for an on-board re-liquefaction system did not perform a comparative study for different types of liquefaction processes that can be applied for a LP gas injection engine for LNG carriers. Second, most of the existing literature focused on the energy efficiency but this approach may miss the effect of the CAPEX that could be a critical point for the realistic adoption of the on-board BOG re-liquefaction system in LNG carrier. Third, the recent rising issue of environmental aspect, in particular CO_2 emissions, were not studied enough.

In this research, two different types of re-liquefaction systems using a LP gas injection engine for LNG carriers are suggested and optimized; no external refrigerant (NER) process and single mixed refrigerant (SMR) process. A comparative analysis is performed with 3 key aspects: energy efficiency, economy, and environment in order to find the optimal technology option for the marine application. In case of efficiency analysis, the total power required for the re-liquefaction system is optimized to investigate the system performance. In the economic analysis, the re-liquefaction system is optimized with total annualized cost as the objective function by estimating the installation cost, operation cost and the cost of cargo loss. A sensitivity analysis with varying LNG price has also been performed in the cost study to identify the feasibility of the re-liquefaction facility under different market situations. In case of environmental analysis, the CO_2 emissions of the main engine, auxiliary engine and GCU are estimated. In addition, we explore how much CO_2 emissions could be reduced through the re-liquefaction system compared to the case without a re-liquefaction system.

2. Modeling, simulation and optimization

2.1. Design basis

The component-level process modeling is carried out by using Aspen HYSYS. Since the re-liquefaction process of BOG occurs under high pressure and cryogenic temperature, the Peng–Robinson equation of state is applied (Peng and Robinson, 1976). Table 1 defines the BOG thermodynamic state and evaporation conditions used in our model. Typically, the temperature of evaporated BOG is higher than that of stored LNG (below −160 °C), and the chemical composition of BOG differs from LNG in the storage tanks by species-dependent evaporation, where the concentration of more volatile components (lower molecular weight, e.g. methane) increases in the BOG stream. The evaporation rate of BOG is assumed to be proportional to the LNG mass stored in the tank with constant heat flux.

The key modeling parameters for the operation of the process equipment are summarized in Table 2. The primary design parts are the fuel gas supply system (FGSS) and the re-liquefaction facility, which include compressors, heat exchangers, and expansion valves. Allowable pressure drops in heat exchanger equipment are assumed from practical values, and non-isentropic fluid flow is assumed during BOG compression and expansion. Two 3600 kW auxiliary engines ($P_{\text{injection}} = 6$ bar, specific fuel oil consumption (SFOC) = 7,590 kJ/kWh) (Wärtsilä, 2019) are assumed to produce electricity with 50% load. For vessel propulsion, two 11,620 kW low-pressure ($P_{\text{injection}} = 16$ bar, SFOC = 7269 kJ/kWh) gas injection engines are modeled, operating at 40% load (WinGD, 2018).

Table 1
BOG thermodynamic state and evaporation conditions (Romero Gómez et al., 2015; Shin and Lee, 2009; Lee et al., 2014; Cha et al., 2018).

Parameters	Unit	Value
BOG property		
Pressure	bar	1.06
Temperature	°C	−120
BOG Composition		
Nitrogen	mol %	0.48
Methane	mol %	99.49
Ethane	mol %	0.03
BOG generation		
Boil-off rate	vol %/day	0.1
Tank Volume	m^3	170,000
LNG Liquidity	vol %	0.95
LNG Density	kg/m^3	437.89

Table 2
Modeling parameters of the process equipment (Wärtsilä, 2019; WinGD, 2018).

Parameter	Unit	Value
Compressor isentropic efficiency	%	75
Intercooler outlet temperature	°C	45
Intercooler ΔP	bar	0.5
Heat exchanger ΔT_{min}	°C	3
Heat exchanger ΔP	bar	0.03-0.5
Auxiliary engine power	kW	3,600
$SFOC_{AUX}$	kJ/kWh	7,590
Propulsion engine power	kW	11,620
$SFOC_{PROP}$	kJ/kWh	7,269

2.2. No external refrigerant (NER) process

A schematic of the process flow diagram including fuel gas supply system (FGSS) with total recycle and no external refrigerant (NER) re-liquefaction is presented in Fig. 1. This scheme utilizes generated BOG from the LNG tank as a refrigerant. In this cycle, the BOG generated from the tank (B1) is firstly compressed (K-1) and cooled by an intercooler (IC-1). A portion of the low-range pressure BOG (B7) is compressed and sent to the auxiliary engine (P = 6 bar, T = 45 °C). Most of the remaining BOG, except the part burnt in the GCU (B6), is transferred to stream B8 for propulsion use. The BOG fuel supplied to the propulsion engine is again compressed and cooled down to the engine intake condition (P = 16 bar, T = 45 °C). The remaining BOG exceeding the engine flowrate (B15) is compressed to the operating pressure for the re-liquefaction process and recycled. The compressor outlet pressure (B16) is chosen as an optimization variable, where the upper bound of compression ratio is set at 4 ($P \leq 64$ bar). Prior to being expanded for phase separation, the re-liquefaction stream (R1) is cooled in the cryogenic heat exchanger (CHE) by heat-exchanging with B2 and R9. The liquified BOG, after a series of expansions (VLV-1, VLV-2), is recovered and sent to the LNG storage tank, while the gas-phase fluid is collected and mixed with the fresh BOG. To reduce the power consumption in the compressors, the gas-phase fluid discharged from phase-separator-1 (R10) is compressed after the CHE, instead of being mixed with B2 before heat recovery.

A different version of the process diagram using NER re-liquefaction with partial recycling is presented in Fig. 2. The purpose is to investigate the benefits of recycling flash gas. The primary difference of the process flow diagram suggested in Fig. 2 is the post-treatment of vent gas after the phase separator. That is, in the re-liquefaction cycle the BOG stream from the phase-separator (R10) is burnt in the GCU without recirculating in the FGSS. Recall that the corresponding gas stream is recirculated (R10) to the fresh BOG stream in Fig. 1. The vent stream transferred to the GCU is in fact a loss, but the total CAPEX may be reduced when adopting the simpler design of a conventional GCU

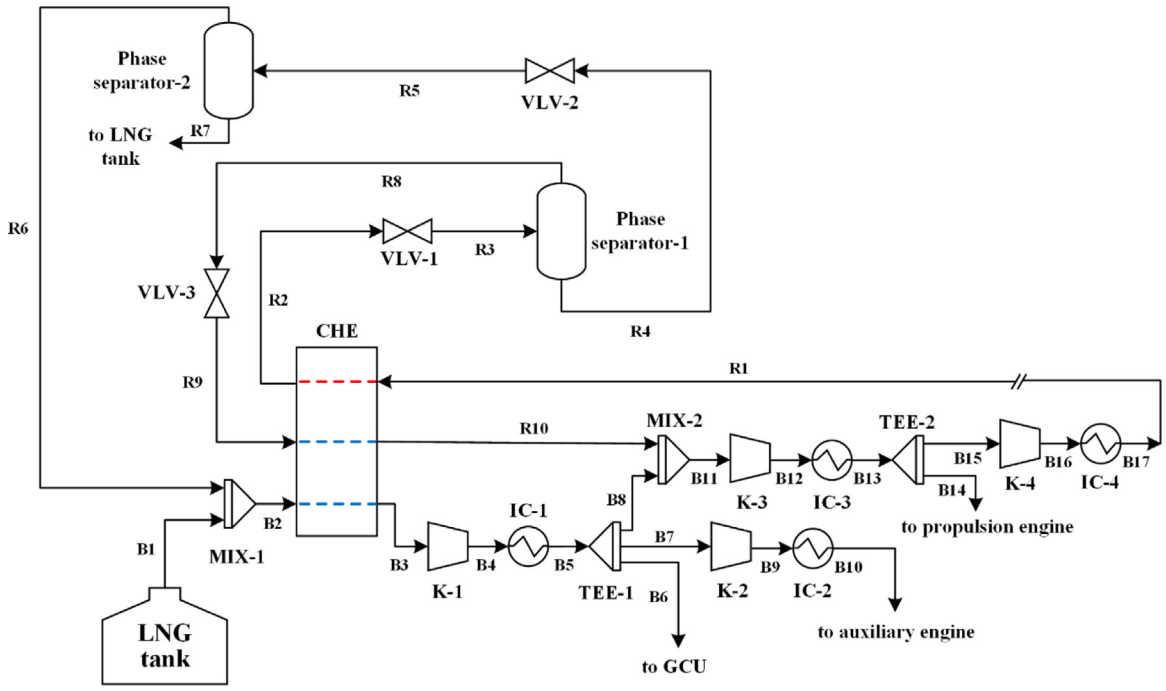

Fig. 1. Process flow diagram for the fuel supply system with total recycle and no external refrigerant for BOG re-liquefaction.

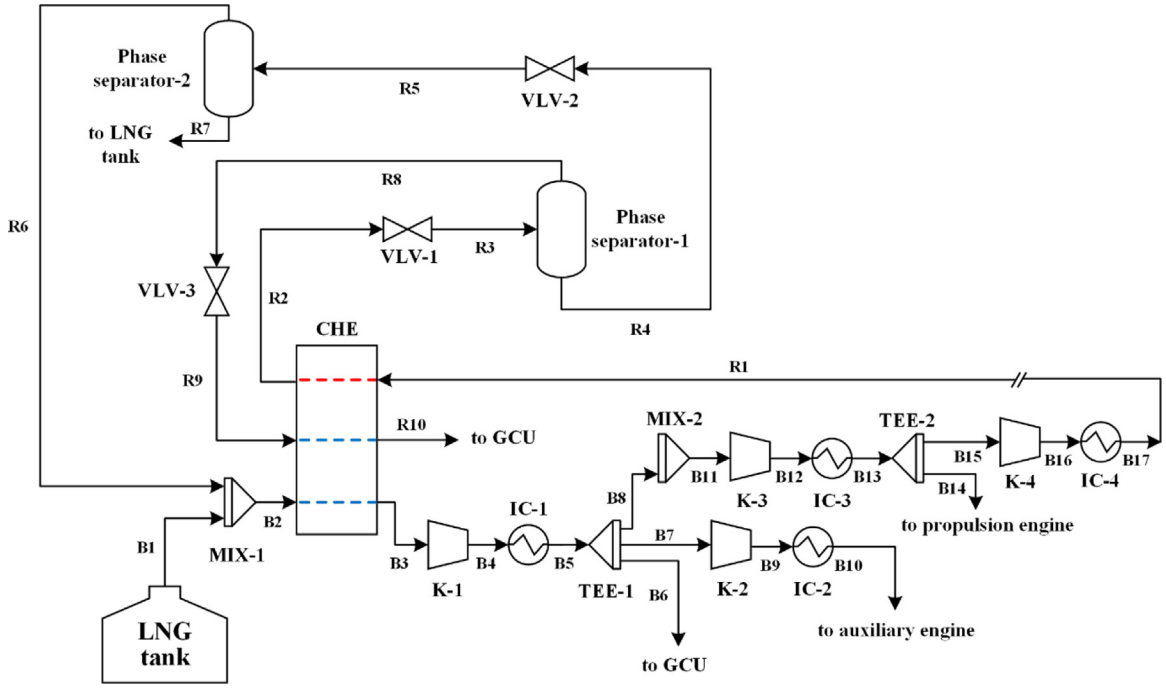

Fig. 2. Process flow diagram for the fuel supply system with partial recycle and no external refrigerant for BOG re-liquefaction.

system and partial recycling. This implies that there exists an optimum point balancing the trade-off between overall system efficiency and capital investment.

2.3. Single mixed refrigerant (SMR) process

A schematic of the process flow diagram utilizing external refrigerant is shown in Fig. 3. In the cycle with mixed-refrigerant (MR), the operation of the refrigerant (MR composition, temperature) is independent of the BOG condition, offering concise control over the re-liquefaction loop. Before the heat is transferred from BOG (B14) to refrigerant (R7), parts of the flow generated from the LNG tank is sent to the generator engine and the propulsion engine. The constituents of the fuel gas supply system are identical to those described in Section 2.1. The surplus BOG (B12) is compressed to a higher pressure (K-4) and cooled (IC-4) to 45 °C before heat-exchange occurring in the CHE. To investigate the influence of feed gas pressure, the maximum compressor outlet pressure in K-4 is set at 16, 40 and 64 bar for our simulation study (in case of 16 bar, feed gas bypasses compressor K-4). The MR cycle is a single-loop refrigeration cycle composed

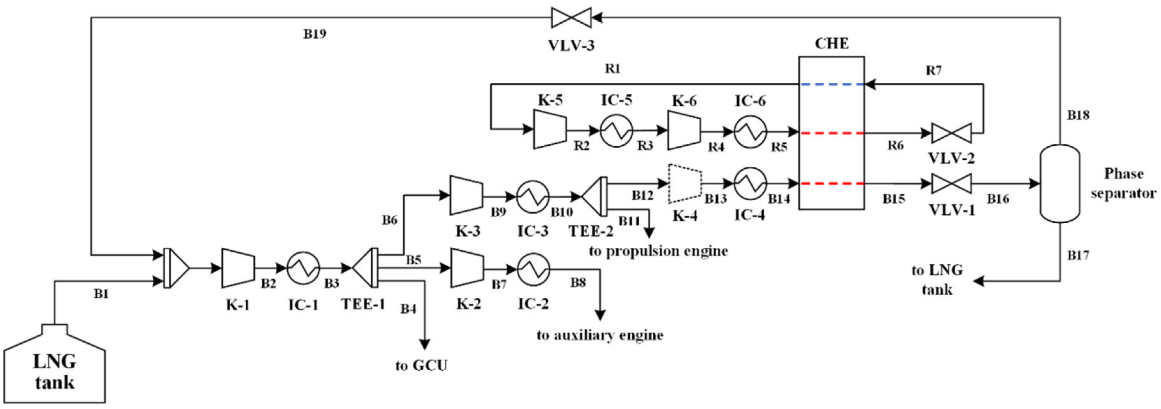

Fig. 3. Process flow diagram for the fuel supply system with SMR cycle for BOG re-liquefaction.

Table 3
Classification of simulation cases.

Case no.	Process type	Maximum feed gas pressure
1	NER total recycle	64
2	NER partial recycle	40
3	NER partial recycle	64
4	SMR	16
5	SMR	40
6	SMR	64

Table 4
Bounds for the decision variables.

Variable	Unit	LB	UB
$\dot{m}_{gcu}$	kg/h	0	1030
Pr_{k-4}	–	1.1	4
Pr_{k-5}	–	1.1	4
Pr_{k-6}	–	1.1	4
T	°C	−160	−90

of a two-stage compressor (K-5 and K-6) and an expansion valve that maximizes the generation of cold duty for BOG cooling. The resulting BOG temperature after the CHE is in the range from −150 to −130 °C depending on the K-4 outlet pressure. The vent stream (B18) is determined by the gas–liquid fraction after cooling and expansion (B16).

In this work, the two re-liquefaction systems (NER and SMR) have been simulated with varying BOG compression levels. This is shown in Table 3, and the case numbers will be used in the following sections unless otherwise noted. Compression of BOG can reduce the liquefaction energy of the methane-rich gas. However, depending on the pressure level, it will result in a larger number of compression stages, taking larger CAPEX and space. Therefore, different maximum pressure levels of the compressed BOG are tested to evaluate this trade-off. Accordingly, the optimization is carried out by dividing the cases into six distinct simulations as shown in Table 3.

2.4. Optimization

The optimization were performed to minimize the specific power consumption (*SPC*) and the total annualized cost (*TAC*) with the decision variables **x** as seen in Eq. (1).

$$\begin{aligned} &\min_{\mathbf{x}} f(\mathbf{x}) = SPC, TAC \\ &\text{subject to} \quad \Delta T_{\min,\mathrm{CHE}} \geq 3 \\ &\qquad\qquad \mathbf{x}_{LB} \leq \mathbf{x} \leq \mathbf{x}_{UB} \end{aligned} \tag{1}$$

The mass flow rate of the BOG sent to the GCU were set as key variable, which affects the capacity of the re-liquefaction system. By considering operating issues, the system was optimized by varying the pressure ratio of compressors (K-4, K-5 and K-6) from 1.1 to 4. Since the temperature at the end of the heat exchanger is an important variable that affects the system, the optimum value was found in the range of −160 °C to −90 °C. In case of SMR, the composition of the mixed refrigerant and the mass flow rate were also set as an variable. A minimum temperature difference of 3 K in the heat exchanger is applied to constrain the processes.

Particle swarm optimization (PSO) is applied for energy efficiency and cost optimization of the re-liquefaction system because it shows robust performance with a constrained liquefaction process (Na et al., 2017). PSO is a stochastic search algorithm being capable of solving non-linear optimization problems in a heuristic manner. Based on the mechanisms of swarming or collaborative behavior of biological populations, the PSO uses a population-based search method where a set of randomly generated solutions propagates in the shared design space towards the optimal solution over a number of iterations (see Table 4).

3. Key performance indicators

The suggested re-liquefaction process systems with NER and SMR are analyzed from three perspectives: energy efficiency, economy and environment. In the efficiency and economy sections, optimization is performed and the background and method for selecting objective functions are described. The environmental part provides a detailed explanation of how CO_2 emissions are calculated in this study.

3.1. Energy efficiency

In a liquefaction process, energy efficiency is one of the most critical factors when evaluating the overall system performance. The primary objective of on-board LNG re-liquefaction facilities is to recover the generated BOG to avoid burning the gas in the GCU. To simplify the analysis of system efficiency, the specific power consumption (*SPC*) is used as an objective function. *SPC* is defined as the power consumption (kW) divided by the amount of recovered LNG (kg LNG) that sent to storage tank, see Eq. (2).

$$SPC = \frac{P_{\text{power consumption}}}{\dot{m}_{\text{re-liquefied LNG}}} (\text{kWh/kg LNG}) \tag{2}$$

3.2. Economical aspects

With the recent trend towards mounting re-liquefaction systems on LNG carriers, it is necessary to analyze the cost of the

Table 5
Factors and coefficients for capital cost calculation (Turton, 2013).

Equipment	A	Type	K_1	K_2	K_3	F_{BM}
Compressor	Power [kW]	Reciprocating	2.2897	1.3604	−0.1027	7.0
Heat exchanger	Area [m^2]	Plate fin	4.6656	−0.1557	0.1547	4.3
Intercooler	Area [m^2]	Shell and tube	2.7652	0.7282	0.0783	3.3–8.8
Phase separator	Volume [m^3]	2 phase vertical	3.4974	0.4485	0.1074	10.3–36.9

system as to whether the re-liquefaction system could bring economic benefits. From the ship's point of view, the purpose of the LNG carrier is to transport the product (LNG) to its destination. If the cost of the re-liquefaction facility is greater than the value of the recovered LNG, the motivation for the installation of a re-liquefaction process is weakened. In this study, total annualized cost (TAC) of the re-liquefaction system together with the lost value of the unrecovered BOG is used as the objective function, see Eq. (3).

$$TAC = ATCI + ATOC + C_{\text{BOGloss}} \tag{3}$$

$ATCI$ and $ATOC$ are annualized capital investment and annual operating cost, respectively. C_{BOGloss} reflects the cost associated with the BOG loss, including the loss of cargo (LNG) from the storage tank during unloading and voyage. The installation of a re-liquefaction facility can reduce C_{BOGloss} while investment cost increases.

The annualized total capital investment ($ATCI$) is estimated from the total capital investment (TCI) of the facility and equipment (Turton, 2013)

$$TCI = F_{\text{Ext}} \sum_j C_{\text{P}}^j F_{\text{BM}}^j \tag{4a}$$

$$ATCI = TCI \left(\frac{i(1+i)^n}{(1+i)^n - 1} \right) \tag{4b}$$

Eq. (4a) shows that TCI is calculated by summing the individual costs of the equipment. The cost of a single equipment j (e.g., compressor) is the product of the initial purchased cost of the item (C_p) and a weighting factor (F_{BM}) that is associated with the equipment installation and related costs. An extra weighting factor ($F_{ext} = 1.18$) is considered for TCI calculation in Eq. (4a). In particular, the purchased cost C_p is estimated using Eq. (5) (Turton, 2013)

$$C_{p,j} = K_{1,j} + K_{2,j} \cdot \log_{10} A_j + K_{3,j} \cdot \left(\log_{10} A_j\right)^2 \tag{5}$$

where K_1, K_2, and K_3 are equipment-specific coefficients and A is the capacity of unit j. The values for F_{BM} and K required for the cost estimation are summarized in Table 5. Based on the TCI obtained from Eq. (4a), the $ATCI$ is assessed in Eq. (4b) assuming a finite service lifetime of the vessel ($n = 20$ yrs.) and a fixed annual rate ($i = 10\%$).

The annual total operating cost ($ATOC$) is calculated by summing the costs associated with the maintenance and operations. The expression for $ATOC$ is given by Eq. (6).

$$ATOC = F_{\text{CTO}} ATCI + (C_e \sum P_{\text{comp}} + C_{\text{cw}} \sum D_{\text{cw}}) \tag{6}$$

where F_{CTO} is a factor for the maintenance and supply that is proportionally increasing with the annualized initial capital investment, and C_e and C_{cw} are the unit price of electricity and cooling water required for the operation of the intercooler, respectively. For this work, F_{CTO} is assumed to be 0.066.

Finally, the economic loss from the unrecovered BOG is expressed in Eq. (7).

$$C_{\text{BOGloss}} = C_{\text{LNG}} N_{\text{cycle}} \sum E_{\text{BOG}}^j t^j \tag{7}$$

where C_{LNG}, N_{cycle}, E_{BOG}, and t represent the unit cost of LNG (in \$/MMBTU), the frequency of the voyage, the rate at which BOG is generated in mode j (in the unit of equivalent heat energy, MMBTU/day), and the elapsed time for mode j (in days), respectively. For the summation on the right-hand side of Eq. (7), two types of modes are considered for the BOG losses; (1) during the voyage and (2) unloading. For this work, the annual operation frequency (N) is assumed to be 11. The time required for voyage (15 days) and unloading (0.5 day) is calculated for a vessel speed of 12 kts.

Table 6
Thermodynamic state of the combustion chamber.

	Pressure	Temperature	Air-excess ratio
GCU	1 bar	300.4 K	1.1
Engine	32 bar	470.9 K	1.0

3.3. Environmental aspects

The environmental regulation regarding greenhouse gas and pollutants emitted from a vessel is becoming a major issue in the LNG process design methodology. Despite the benefit of re-liquefaction systems to recover surplus BOG, these systems inevitably require and consume electrical power primarily in the pressure boosting compressor stage. Thus, it is essential to evaluate the environmental impact of the re-liquefaction system in conjunction with efficiency and economic feasibility. In order to be consistent with the international protocols (Energy API, 2015) assessing the environmental aspects of LNG carriers, the amount of carbon dioxide (CO_2) emitted from a vessel is chosen as the major environmental factor. The direct source of the additional CO_2 caused by the re-liquefaction process is the auxiliary engine, that supports power requirements of the compressors. In this work, the CO_2 production caused by the engine is calculated using a numerical kinetic simulation code based on the open-source software Cantera with a detailed GRI 3.0 reaction mechanism (Frenklach et al., 2021). While the typical CO_2 calculation assumes that all carbon in the fuel is completely converted to CO_2, the method used here can allow for the consideration of both fuel chemistry and firing configuration. The GRI-Mech 3.0 is a widely accepted kinetic model optimized for CH_4 combustion, which contains 53 species and 325 elementary reactions.

In this work, a code written in Matlab interface is used to run the Cantera software library and analyze the equilibrium composition of the target mixture. Table 6 summarizes the thermodynamic state of the combustion chamber for the kinetic simulation.

The numerical solver yields the product gas compositions (Y_i) at which the Gibbs energy of the mixture is minimized. The resulting CO_2 concentration in the exhaust gas is calculated by the element potential method (Camberos and Moubry, 2001). The mass flow of CO_2 can be calculated by Eq. (8).

$$\begin{aligned} \dot{m}_{\text{CO}_2} &= \dot{m}_{\text{CO}_2,\text{PROP}} + \dot{m}_{\text{CO}_2,\text{AUX}} + \dot{m}_{\text{CO}_2,\text{GCU}} \\ &= Y_{\text{CO}_2,\text{engine}} \left[\dot{m}_{\text{GAS,PROP}} + \dot{m}_{\text{GAS,AUX}} \right] + Y_{\text{CO}_2,\text{GCU}} \dot{m}_{\text{GAS,GCU}} \end{aligned} \tag{8}$$

where $Y_{CO_2,engine}$ depends on the fuel composition, inlet gas temperature, pressure, and the geometrical characteristics of the engine (e.g., compression ratio of the two-stroke engine) being used.

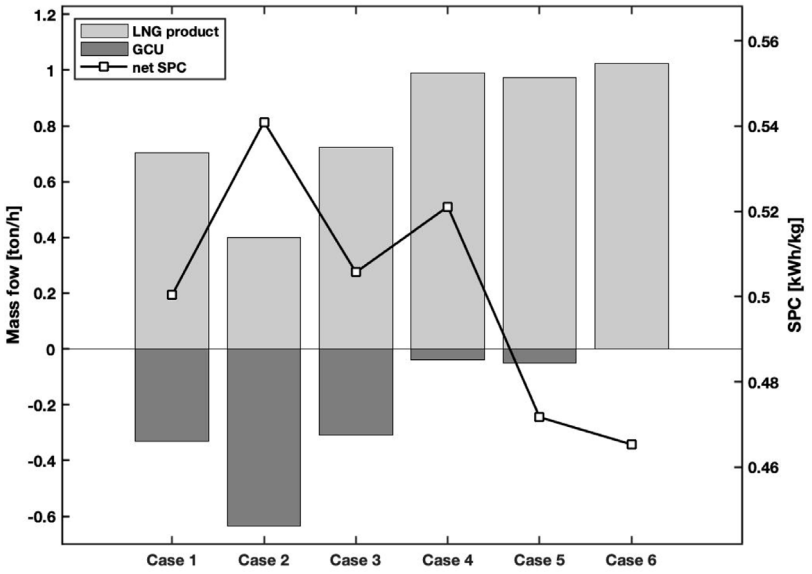

Fig. 4. Results from energy efficiency optimization.

Table 7
Results from energy efficiency optimization.

Case		Max. feed gas pressure	Re-liquefaction ratio[a]	*SPC*	Power	GCU	LNG product
		bar	%	kWh/kg	kW	kg/h	kg/h
1	NER total recycle	64	74	0.5004	351.6	330.7	702.5
2	NER partial recycle	40	74	0.5410	215.8	634.9	398.8
3	NER partial recycle	64	74	0.5057	366.1	309.6	723.9
4	SMR	16	97	0.5211	515.4	37.7	989.1
5	SMR	40	77	0.4717	458.6	51.0	972.2
6	SMR	64	81	0.4653	476.0	0.0	1023.1

[a] $Re-liquefaction\ ratio = \frac{re-liquefied\ BOG}{surplus\ BOG}$.

Table 8
Refrigerant composition results from energy efficiency optimization.

	Unit	Case 4	Case 5	Case 6
Nitrogen	mol %	11.9	4.7	7.7
Methane	mol %	44.0	44.5	37.0
Ethane	mol %	20.3	26.3	30.8
n-Butane	mol %	23.8	24.6	24.5

A constant volume reactor model is applied for engine combustion, unlike the constant pressure reactor applied for the GCU. During combustion, it is assumed that there is no turbulence effect and heat-loss of the mixture caused by flame radiation and wall diffusion. Exhaust gas recirculation is not considered. To calculate thermodynamic properties (such as specific heat, enthalpy, and entropy) at different temperatures, the Burcat's database (Burcat, 2021) and NASA 9-coefficient polynomial format McBride et al. (2002) are applied. The equilibrium state of element potential minimization is solved using Villars–Cruise–Smith stoichiometric algorithm (Wong, 2001).

4. Results and discussion

4.1. Energy efficiency

Fig. 4 and Tables 7, 8 show the results of energy efficiency optimization measured in specific power consumption (*SPC*). When compared with other studies and patents having *SPC* from 0.28 to 0.42 kWh/kg (Tan et al., 2016, 2018; Kwak et al., 2018; Bahram Ghorbani et al., 2018), all six cases showed lower *SPC*. Since the engine supply pressure is relatively low, additional feed gas compression is required for efficient re-liquefaction. Also, unlike previous studies (Tan et al., 2016, 2018; Kwak et al., 2018; Bahram Ghorbani et al., 2018), the liquefaction target of this study is BOG, and the fact that it is a component close to pure methane is also the reason for low efficiency. The BOG re-liquefaction ratio, shown in the unit of percentage (%), represents the portion of BOG recovered during the re-liquefaction process at steady-state. When no external refrigerant is used (Cases 1 to 3), the re-liquefaction ratio is quite low at 74%, compared to the mixed refrigerant cases. Cases 4 to 6 that exhibit much higher BOG re-liquefaction ratio (77%–97%). This is partially owing to the lower upper limit of refrigerant pressure (64 bar) for the NER process. For engines with higher-injection-pressure such as MEGI, the Joule–Thomson fluid expansion occurs at nearly 300 bar, so a higher re-liquefaction ratio is possible. The precooling of the BOG stream in the NER process is limited by the BOG temperature from the LNG tank (−120 °C in this study), so a further reduction is hard to achieve without external refrigerants, considering small temperature drops across JT valves with a relatively low upper limit on refrigerant pressure. On the other hand, the SMR process can achieve higher BOG re-liquefaction ratio since it can independently supply a lower temperature MR, reaching the BOG temperature at the point of maximum re-liquefaction ratio prior to expansion. As a result, at the optimal point, the *SPC* is estimated at 0.50–0.54 for the NER process, whereas the range of *SPC* for the SMR process is from 0.47 to 0.52 varying with the feed pressure. It is noteworthy that the *SPC* of the NER process becomes lower when some fraction of the BOG stream is sent to the GCU. This reveals that while the absolute amount of recovered LNG product becomes less for the NER process, combining the

GCU with BOG recovery can be a more strategic approach in terms of the efficiency for identical expansion pressures, although the use of the GCU has detrimental effect on the environmental evaluation. When the BOG pressure is decreased to 40 bar for the NER process, both the efficiency (*SPC*) and net amount of LNG recovered are significantly degraded due to the reduced JT cooling effect. On the other hand, the SMR process provides lower *SPC* than that of the NER process, and higher pressure of the inlet BOG reduces the *SPC*. The BOG has a relatively high content of methane compared to the natural gas mixture, which makes the cooling curve of the hot streams in the CHE having a more horizontal line during phase change, as shown in Fig. 5. This reduces the heat exchange efficiency. With higher pressure of the BOG, the range of this horizontal line decreases since the phase envelope becomes narrower with higher pressure, and this makes the heat exchange more efficient. The LMTD (log mean temperature difference) for Case 4, Cases 5 and 6 are quite similar, 5.59, 5.40 and 5.26 respectively. However, exergy loss of heat exchanger for Case 6 (0.41 MW) are 48% lower than Case 4 (0.61 MW) and 11% lower than Case 5 (0.46 MW). It should be mentioned though, that exergy losses depend on both the driving forces (e.g. LMTD) and the absolute temperature. Below ambient, exergy losses increase rapidly with lower temperatures for the same temperature difference. This is the main reason why Case 6 performs better than Case 4 and Case 5 due to the smaller temperature difference in the colder region of the heat exchanger. Besides, for Case 6, the required BOG temperature before JT expansion for re-liquefaction becomes higher, which reduces cooling of the MR.

4.2. Economical evaluation

Fig. 6 and Tables 9, 10 shows the economic optimization results of each system when the LNG cost is $5/MMBTU. The results show that the optimal points of Cases 1 and 3 (NER process) include burning around 300 kg/h of the BOG in the GCU. This is due to the limited available energy for re-liquefaction in NER process. To increase the re-liquefaction flow rate, a larger flow rate must be recycled from the separator. Increased flow rate of the recycle stream means an increase in the capacity of the equipment, which leads to higher capital cost. Likewise, when the maximum compression pressure of the feed gas is limited to 40 bar (Case 2), less cold energy is available for heat exchange compared with that of 64 bar (Case 3). Due to this smaller cooling capacity, the best option is found to be a larger flow through the GCU at about 635 kg/h.

For Case 4 (SMR with maximum 16 bar pressure), burning the entire surplus BOG in the GCU is more economical than to recover LNG through the re-liquefaction system. As explained in Section 4.1, at low BOG pressure, more flow rate of MR is required, which leads to an increase in energy consumption and the size of the MR compressor and the cryogenic heat exchanger. This makes the cost of the re-liquefaction system larger than the economical benefits from the recovered LNG. Despite the higher BOG losses, in this case a better decision is to not install a re-liquefaction system. On the other hand, Cases 5 and 6 (SMR with 40 and 64 bar pressure limitation) show that recovering LNG through a re-liquefaction system is a better option to reduce cost. Despite the increase in power consumption of the feed gas compressor, Cases 5 and 6 show about 1.6 and 4.2% lower *TAC* than Case 4. This is possible due to the lower *SPC* with higher BOG pressure, as explained in Section 4.1. This consequently leads to a decrease in the flow rate of the MR cycle, and thereby reducing the OPEX of the MR compressor.

When comparing the NER process with the SMR process, the NER process shows around 10% less *TAC*. This is because the NER process has an optimum allowable capacity, so it should burn some BOG in the GCU. SMR processes have higher *TAC* due to the additional compressors, larger heat exchanger, and additional

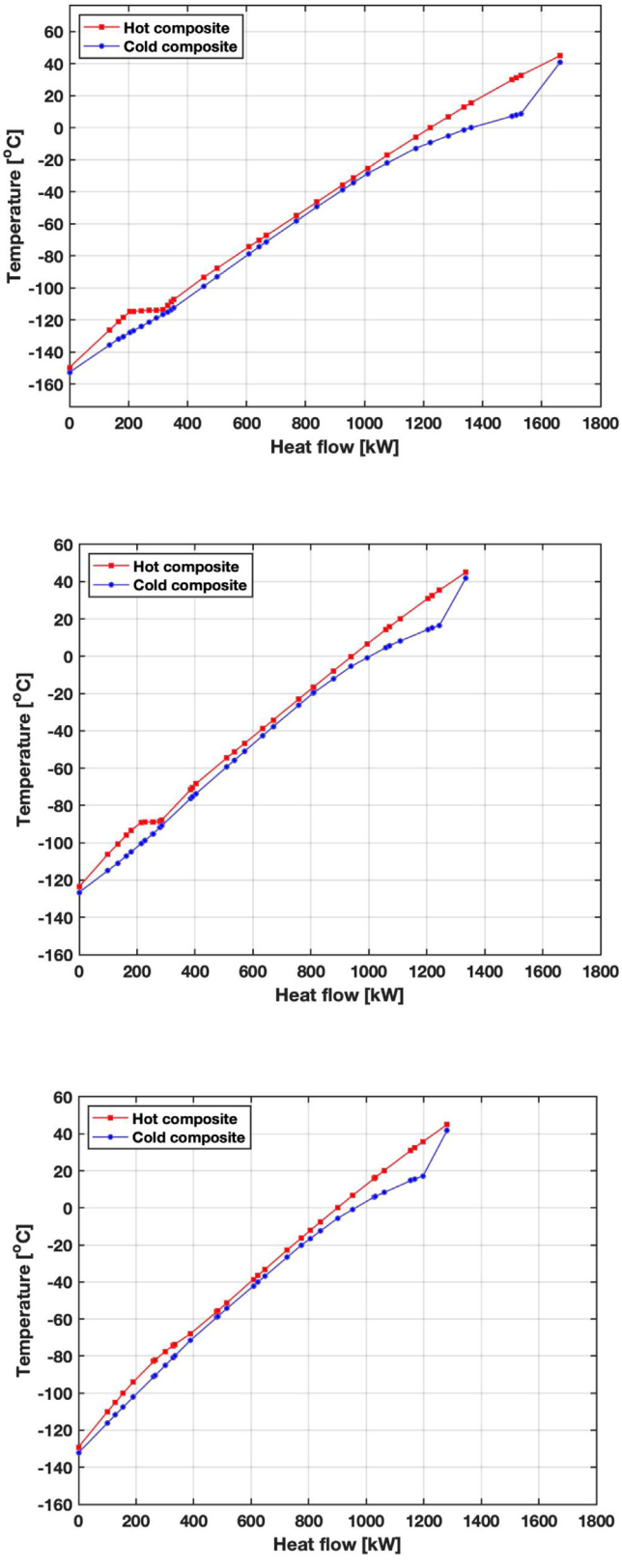

Fig. 5. Temperature-Heat flow diagram of Cases 4 to 6.

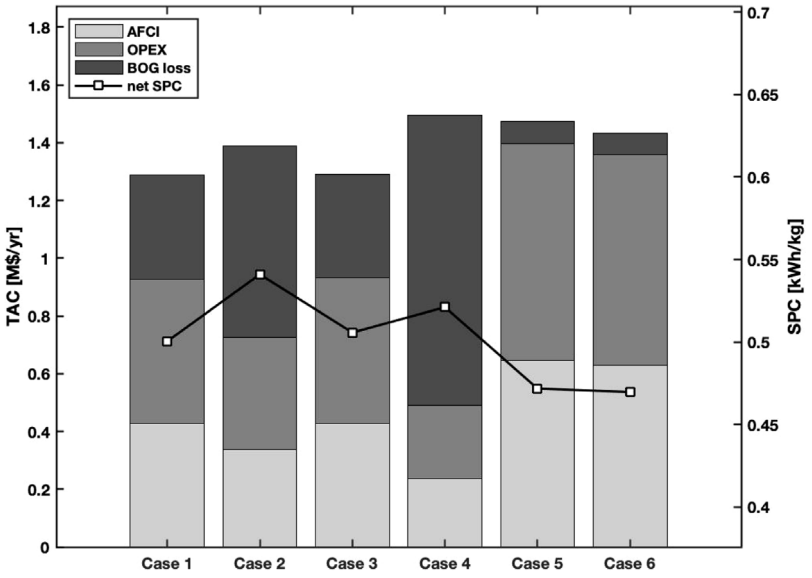

Fig. 6. Optimization results based on economical analysis.

Table 9
Optimization results from the economical analysis.

		Unit	Case 1	Case 2	Case 3	Case 4	Case 5	Case 6
Re-liquefied LNG		kg/h	726.8	398.3	726.2	–	1023.6	1023.9
GCU		kg/h	306.3	635.4	307.3	1028.8	0.1	0.1
Power consumption		kW	368.5	216.8	371.3	–	548.3	520.3
Specific power		kWh/kg	0.5071	0.5443	0.5113	–	0.5356	0.5081
CHE	Cold duty	kW	200.1	112.6	199.4	–	1092.7	986.7
	UA	kW/C	21.8	9.2	22.0	–	113.4	110.6
	LMTD	C	9.2	12.3	9.0	–	9.6	8.9
	ΔT_{min}	C	3.0	3.0	3.0	–	3.0	3.0
	Outlet T	C	−117.8	−118.9	−118.2	–	−134.5	−137.8
TCI	Compressor	k$	2822.13	2254.48	2832.02	1798.96	3825.13	3725.40
	CHE	k$	547.94	402.05	550.18	–	1302.49	1282.35
	Intercooler	k$	213.95	176.04	214.41	162.12	320.39	305.05
	Separator	k$	44.51	44.51	44.51	–	44.51	44.51
	Total	k$	3628.54	2877.08	3641.11	1961.08	5492.51	5357.30
ATCI		k$/yr	426.21	337.94	427.68	235.33	645.15	629.27
ATOC		k$/yr	502.07	386.80	504.14	254.26	752.68	730.00
BOG loss		k$/yr	359.58	665.00	358.64	1005.54	74.38	74.37
TAC		k$/yr	1287.86	1389.74	1290.46	1495.14	1472.21	1433.65

Table 10
Refrigerant composition results from economical analysis.

	Unit	Case 4	Case 5	Case 6
Nitrogen	mol %	–	4.1	6.3
Methane	mol %	–	45.3	35.7
Ethane	mol %	–	25.4	31.8
n-Butane	mol %	–	25.2	26.3

compression energy for the MR. However, it can fully re-liquefy BOG to minimize BOG losses in the GCU.

4.3. Sensitivity analysis

Considering the fluctuations in the LNG price over the past 3 years, a sensitivity analysis is conducted in the range of LNG price between $4/MMBTU and $6/MMBTU, see Fig. 7 and Table 11. The change in LNG price impacts the $C_{BOGloss}$ value, and therefore the point of minimum *TAC* can also be affected, as shown in Table 8.

First, as described above, the NER process (Cases 1 and 3) have an optimal capacity of liquefaction (726.8 kg/h and 726.2 kg/h respectively) when the LNG price is $5/MMBTU. When the BOG price decreases to $4/MMBTU, more combustion in the GCU is advantageous, so the optimum point changes to 495.6 kg/h and 703.8 kg/h respectively. Conversely, when the LNG price is $6/MMBTU, the loss from burning the BOG increases, so the optimal capacity of the re-liquefaction facility is increased to 746.4 kg/h and 743.1 kg/h respectively to reduce the amount burnt in the GCU.

For Case 2, the results show that the optimal capacity of the re-liquefaction system does not change significantly with the LNG price. When the maximum compression is lowered to 40 bar, it leads to a decrease in the JT cooling effect, and the maximum capacity is 398.3 kg/h when the LNG price is $5/MMBTU, which is small compared to Case 1 (726.8 kg/h) and Case 3 (726.2 kg/h). Therefore, even if the LNG price rises to $6/MMBTU, it is difficult to re-liquefy a larger amount of BOG, so there is little change in capacity (401.5 kg/h).

For the SMR process, when the LNG price is $4/MMBTU, the optimal point is where the entire amount of BOG is burnt in the GCU, since the costs of installing a re-liquefaction system become higher than the BOG losses, similar to Case 4 with

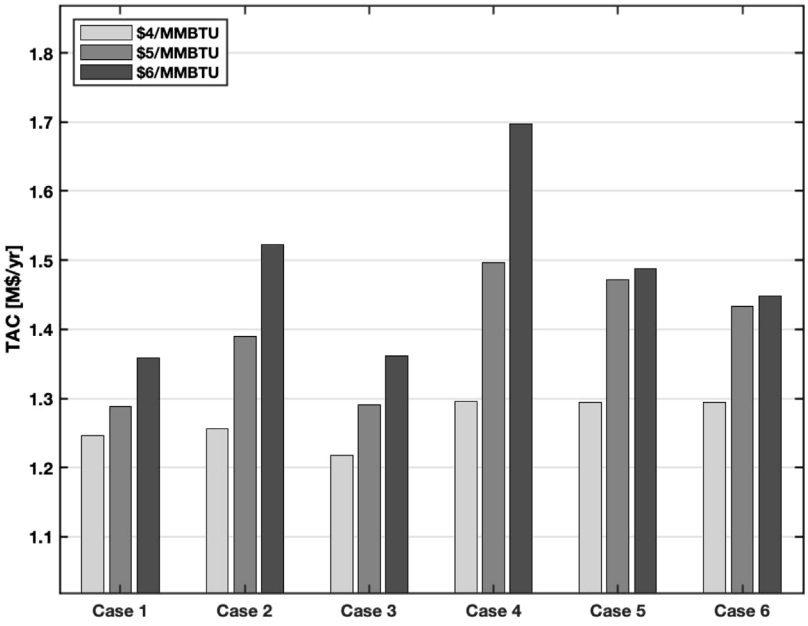

Fig. 7. Sensitivity analysis according to LNG price.

Table 11
Optimization results from the sensitivity analysis.

Case	LNG price	re-liquefied LNG	GCU	*ATCI*	*ATOC*	BOG loss	*TAC*
	$/MMBTU	kg/h	kg/h	k$/yr	k$/yr	k$/yr	k$/yr
Case 1	4	495.6	537.0	361.84	425.21	459.48	1246.53
	5	726.8	306.3	426.21	502.07	359.58	1287.86
	6	746.4	286.9	434.01	514.57	409.78	1358.36
Case 2	4	397.8	635.8	337.79	386.52	532.33	1256.65
	5	398.3	635.4	337.94	386.80	665.00	1389.74
	6	401.5	632.1	339.34	389.08	794.37	1522.80
Case 3	4	703.8	329.6	419.03	494.40	303.62	1217.05
	5	726.2	307.3	427.68	504.14	358.64	1290.46
	6	743.1	290.5	434.46	515.26	411.47	1361.20
Case 4	4	0.0	1028.8	235.33	254.26	804.43	1294.02
	5	0.0	1028.8	235.33	254.26	1005.54	1495.14
	6	0.0	1028.8	235.33	254.26	1204.20	1693.79
Case 5	4	0.0	1028.8	235.33	254.26	804.43	1294.02
	5	1023.6	0.1	645.15	752.68	74.38	1472.21
	6	1023.4	0.0	644.71	754.16	89.18	1488.05
Case 6	4	0.0	1028.8	235.33	254.26	804.43	1294.02
	5	1023.9	0.1	629.27	730.00	74.37	1433.65
	6	1023.4	0.1	628.48	730.87	89.26	1448.60

$5/MMBTU. However, at higher prices ($5/MMBTU, $6/MMBTU), it is beneficial to recover LNG by operating the re-liquefaction system. Compared to the NER process, the flow rate to the GCU is small, so the variation in *TAC* is relatively small with the LNG price.

4.4. Environmental analysis

Fig. 8 shows the amount of CO_2 emitted in Cases 1 to 6 and the reference case. The reference case shows the amount of CO_2 generated when all surplus BOG is combusted in the GCU rather than using a re-liquefaction system. The sources of ship CO_2 emissions are divided into 3 types: the propulsion engine, the auxiliary engine, and the GCU. Through comparison with the reference case, the operation of a re-liquefaction system could reduce cargo loss as well as reduce CO_2 emissions. The results show that the SMR process (Cases 5 and 6) emits 15% less CO_2 than the NER process (Cases 1 and 3). This indicates that it is environmentally beneficial to reduce the use of the GCU by increasing the capacity of the re-liquefaction system. Compared to the NER process, the SMR process has relatively higher power consumption in the re-liquefaction system, and CO_2 emissions from the auxiliary engine increases ∼10% due to the additional engine load for electricity generation. However, the additional fuel injection that supports operation of the re-liquefaction facility diminishes the fraction of BOG stream burnt in the GCU, thereby achieving substantial reduction in total vessel CO_2 emissions. This implies that the SMR process is advantageous from environmental aspects, but not from economic aspects.

Among the three cases with the NER process, Cases 1 and 3 (64 bar limit) exhibited better environmental performance compared with Case 2 (40 bar limit). Despite the slight increment in auxiliary engine emission in Cases 1 and 3, the total system CO_2 emission is reduced. At the same time, Cases 1 and 3 show better results in terms of total annualized cost compared to Case 2. Therefore, compressing the feed gas is beneficial for the performance of the re-liquefaction system in all aspects.

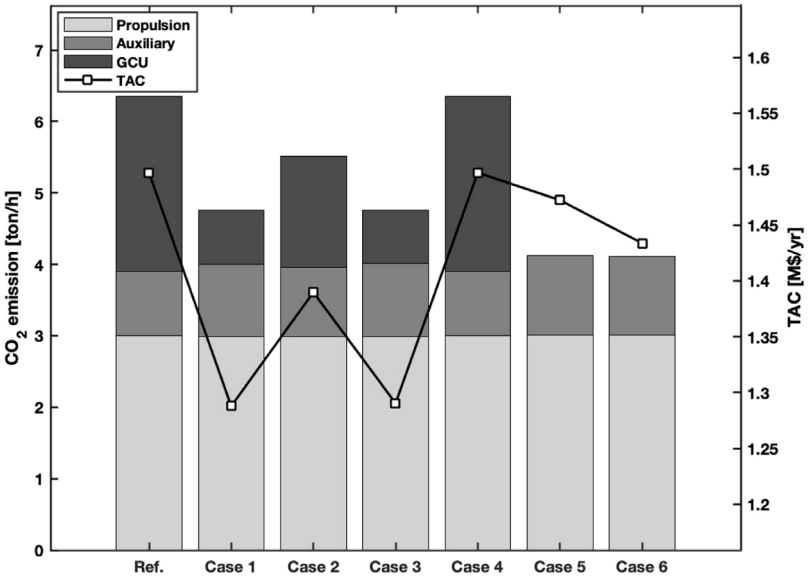

Fig. 8. Breakdown of CO_2 emission.

In the SMR Cases 4 to 6, the high-pressure feed gas (Cases 5 and 6) also show better results. It is noteworthy that the CO_2 emissions show a big difference between Case 4 and Cases 5 and 6. Unlike Case 5 and 6, Case 4 has an optimum point where the entire amount of BOG is burnt in the GCU without operating the re-liquefaction system. As a result, GCU emissions are considerable. However, the CO_2 emissions become slightly reduced at higher pressures. Also, the *TAC* is gradually decreasing with the increment of operating pressure. This means that the system operates more economically at higher pressure conditions; while Case 5 and Case 6 emit nearly the same amount of CO_2.

The ship industry's attention is focused on developing a green ship industry due to intensified environmental regulations. In line with this, using re-liquefaction systems can reduce CO_2 emissions in the natural gas life cycle by reducing the CO_2 emissions from transport. In addition, even if future regulations and CO_2 incentives/tax are not considered, it can bring benefits from an economic point of view. Therefore, a re-liquefaction system could be an attractive option as an intermediate solution on the way to low/zero emission ships (e.g. onboard carbon capture system, H_2, NH_3 ships).

5. Conclusion

This study has analyzed two re-liquefaction systems for an LNG carrier equipped with low pressure gas injection engine from the aspects of energy, economy and environment. The two re-liquefaction systems are (i) no external refrigerant (NER) and (ii) single mixed refrigerant (SMR) cycle. The results of the energy optimization show that the SMR alternative can recover 45% more LNG with 6% less specific power consumption (*SPC*) than the NER process. However, the overall power consumption is 27% higher.

From the economical analysis, the NER process has 10% lower total annualized cost (*TAC*) than the SMR process when the LNG price is \$5/MMBTU. Although the cost of BOG losses in the NER processes is 20% higher than that of the SMR process, the capital cost and operating cost of the SMR are about 45% and 47% higher than for the NER cases. A sensitivity analysis on LNG price performed from \$4/MMBTU to \$6/MMBTU indicates that the NER process is advantageous when the LNG price is low, while the SMR process is advantageous when the LNG price is high.

In the environmental analysis, all cases show that in fact, the installation of an on-board reliquefaction system reduces the CO_2 emissions of LNG carriers. In addition, the SMR process is proven to be a more environment friendly system. The NER process has less power consumption compared to the SMR process, but it requires BOG burning in the gas combustion unit (GCU) due to a limited re-liquefaction capacity. This results in an increase in CO_2 emissions in the NER process, whereas the CO_2 emissions of the SMR process are 14% lower than that of the NER process due to the full liquefaction capability. In conclusion, this study demonstrates that BOG re-liquefaction systems have the potential to be an effective measure to reduce CO_2 emissions in the shipping industry while minimizing cargo loss, which is a valuable economic benefit.

For a more accurate calculation, more detailed operating information should be considered. In addition, some gas injection engines have the issue of a methane slip, which contributes the global warming more severely than carbon dioxides. These effects need to be considered in a future study.

CRediT authorship contribution statement

Chulmin Hwang: Conceptualization, Methodology, Software, Data curation, Writing – original draft, Visualization. **Sungkyun Oh:** Investigation, Software, Data curation. **Donghoi Kim:** Methodology, Software, Writing – review & editing. **Truls Gundersen:** Writing – review & editing, Validation. **Youngsub Lim:** Methodology, Supervision, Writing – review & editing, Funding acquisition.

Declaration of competing interest

The authors declare that they have no known competing financial interests or personal relationships that could have appeared to influence the work reported in this paper.

Acknowledgment

This work was supported by the National Research Foundation of Korea (NRF) grant funded by the Korea government (MSIT) (No. 2021M3H7A102621612).

References

Bahram Ghorbani, R.S., Mehdi, Mehrpooya, Hamedi, Mohammad-Hossein, 2018. Structural, operational and economic optimization of cryogenic natural gas plant using NSGAII two-objective genetic algorithm. Energy 159, 410–428.

Burcat, A., 2021. Ideal Gas Thermodynamic Data in Polynomial Form for Combustion and Air Pollution Use. Available from: http://garfield.chem.elte.hu/Burcat/burcat.html.

Burckhardt Compression AG, Burckhardt Compression AG, 2016. LABY® Compressors Contactless Labyrinth Sealing for Highest Availability.

Camberos, J.A., Moubry, J.G., 2001. Chemical equilibrium analysis with the method of element potentials. In: 39th AIAA Aerospace Sciences Meeting. Reno, NV.

Cha, S., et al., 2018. Experimental analysis of boil-off gas occurrence in independent liquefied gas storage tank. J. Ocean. Eng. Technol. 32, 380–385.

Choi, J., 2018. Development of partial liquefaction system for liquefied natural gas carrier application using exergy analysis. Int. J. Nav. Archit. Ocean Eng. 10 (5), 609–616.

Council of the European Union, 2019. 74th Session of the IMO Marine Environment Protection Committee.

Energy API, 2015. Consistent Methodology for Estimating Greenhouse Gas Emissions.

Fernández, I.A., Gómez, J.R., Gómez, M.R., Insua, Á.B., 2017. Review of propulsion systems on LNG carriers. Renew. Sustain. Energy Rev. 67, 1395–1411.

Frenklach, M., Bowman, T., Smith, G., 2021. GRI-Mech 3.0. Available from: http://combustion.berkeley.edu/gri-mech/version30/text30.html.

George, D.G., Eleftherios, K.D., Chariklia, G.A., 2020. LNG carrier two-stroke propulsion systems: A comparative study of state of the art reliquefaction technologies. Energy 195.

Hwang, C., Lim, Y., 2018. Optimal process design of onboard BOG re-liquefaction system for LNG carrier. J. Ocean. Eng. Technol. 32, 372–379.

IGU, 2020. 2020 World LNG Report.

Kim, D., Hwang, C., Lim, Y., 2019. Process design and economic optimization of boil-off-gas re-liquefaction systems for LNG carriers. Energy 173, 1119–1129.

Kwak, D.-H., Heo, S.-H., Park, S.-J., Seo, J.-H., Kim, J.-K., 2018. Energy-efficient design and optimization of boil-off gas (BOG) re-liquefaction process for liquefied natural gas (LNG)-fuelled ship. Energy 148, 915–929.

Lee, J., Kim, Y., Hwang, S., 2014. Numerical model of heat diffusion and evaporation by LNG leakage at membrane insulation. J. Ocean. Eng. Technol. 28, 517–526.

Man Diesel & Turbo, 2012. ME-GI Dual Fuel MAN B & W Engines a Technical, Operational and Cost-Effective Solution for Ships Fuelled by Gas.

Man Diesel & Turbo, 2013. Propulsion Trends in LNG Carriers Two-Stroke Engines.

McBride, B.J., Zehe, M.J., Gordon, S., 2002. NASA Glenn Coefficients for Calculating Thermodynamic Properties of Individual Species.

Na, Jonggeol, Lim, Y., Han, Chonghun, 2017. A midified DIRECT algorithm for hidden constraints in an LNG process optimization. Energy 126, 488–500.

Peng, D.-Y., Robinson, D.B., 1976. A new two-constant equation of state. Ind. Eng. Chem. Fundam. 15 (1), 59–64.

Romero Gómez, J., Romero Gómez, M., Lopez Bernal, J., Baaliña Insua, A., 2015. Analysis and efficiency enhancement of a boil-off gas reliquefaction system with cascade cycle on board LNG carriers. Energy Convers. Manage. 94, 261–274.

Shin, Y., Lee, Y.P., 2009. Design of a boil-off natural gas reliquefaction control system for LNG carriers. Appl. Energy 86, 37–44.

Tan, H., Shan, S., Zhao, Q., 2018. A new boil-off gas re-liquefaction system for LNG carriers based on dual mixed refrigerant cycle. Cryogenics 92, 84–92.

Tan, H., Zhao, Q., Li, Y., 2016. Enhancement of energy performance in a boil-off gas re-liquefaction system of LNG carriers using ejectors. Energy Convers. Manage. 126, 875–888.

Tu Huan, F.H., Lei, Wei, Zhou, Guoqiang, 2019. Options and Evaluations on Propulsion Systems of LNG Carriers.

Turton, R., 2013. Analysis, Synthesis, and Design of Chemical Processes, fourth ed. Pearson Education, Upper Saddle River, N.J.

Wärtsilä, 2019. Wärtsilä 34DF Brochure. Helsinki, Finland.

WinGD, 2018. Low-Pressure X-DF Engines FAQ. Winterthur, Switzerland.

Wong, F.C.H., 2001. Chemical Equilibrium Analysis of Combustion Products At Constant Volume. University of Toronto, Toronto.